Molecular and Cellular Mechanisms of *Mycobacterium avium*-Induced Thymic Atrophy

Margarida Borges, Palmira Barreira-Silva, Manuela Flórido, Michael B. Jordan, Margarida Correia-Neves and Rui Appelberg

J Immunol 2012; 189:3600-3608; Prepublished online 24 August 2012;
doi: 10.4049/jimmunol.1201525
http://www.jimmunol.org/content/189/7/3600

The Journal of Immunology is published twice each month by
The American Association of Immunologists, Inc.,
9650 Rockville Pike, Bethesda, MD 20814-3994.

Print ISSN: 0022-1767 Online ISSN: 1550-6606.

Molecular and Cellular Mechanisms of *Mycobacterium avium*-Induced Thymic Atrophy

Margarida Borges,*,†,1 Palmira Barreira-Silva,‡,§,1 Manuela Flórido,*,2 Michael B. Jordan,¶,‖ Margarida Correia-Neves,‡ and Rui Appelberg*

Thymic atrophy has been described as a consequence of infection by several pathogens and shown to be induced through diverse mechanisms. Using the mouse model of *Mycobacterium avium* infection, we show in this study that the production of NO from IFN-γ–activated macrophages plays a major role in mycobacterial infection-induced thymic atrophy. Our results show that disseminated infection with a highly virulent strain of *M. avium*, but not with a low-virulence strain, led to a progressive thymic atrophy. Thymic involution was prevented in genetically manipulated mice unable to produce IFN-γ or the inducible NO synthase. In addition, mice with a selective impairment of IFN-γ signaling in macrophages were similarly protected from infection-induced thymic atrophy. A slight increase in the concentration of corticosterone was found in mice infected with the highly virulent strain, and thymocytes presented an increased susceptibility to dexamethasone-induced death during disseminated infection. The administration of an antagonist of glucocorticoid receptors partially reverted the infection-induced thymic atrophy. We observed a reduction in all thymocyte populations analyzed, including the earliest thymic precursors, suggesting a defect during thymic colonization by T cell precursors and/or during the differentiation of these cells in the bone marrow in addition to local demise of thymic cells. Our data suggest a complex picture underlying thymic atrophy during infection by *M. avium* with the participation of locally produced NO, endogenous corticosteroid activity, and reduced bone marrow seeding. ***The Journal of Immunology*****, 2012, 189: 3600–3608.**

Several microorganisms have been shown to cause premature thymic involution (1). How much premature thymic dysfunction impacts on the immune system depends on factors like the age of the individual, the precise mechanisms that caused thymic atrophy, the consequent ability for thymic recovery after the resolution of the infection, and the concomitant existence or not of peripheral lymphocyte depletion (2). When thymic atrophy occurs in parallel with peripheral lymphopenia, the reconstitution of the immune system depends to a great extent on the ability of the thymus to recover its ability to generate new T cells as it has been extensively shown for AIDS patients (3–5). Because several mechanisms have been implicated in infection-induced thymic atrophy and their role varies depending on the microorganism causing infection, determination of which pathways are responsible for thymic atrophy in distinct situations is essential to define strategies to prevent thymic atrophy and/or promote the recovery of thymic function once the infection is controlled.

Even though the thymus undergoes physiologic atrophy with age, T cells are generated and incorporated into the peripheral T cell pool in adulthood, albeit at slower rate than in children (6–9). Thymectomy or thymic dysfunction in early life has been shown to cause premature aging of the immune system in humans (10), as well as enhanced autoimmunity in mice (11). Moreover, loss of thymic activity in adults has been shown to reduce oral tolerance (12) and to hamper the affinity maturation of Abs (13). Loss of thymic T cell output in adults has more obvious consequences when peripheral lymphopenia occurs concomitantly as it is the case in AIDS patients (14).

Several mechanisms have been implicated in infection-induced thymic atrophy. A major role was attributed to corticosteroids because of their ability to cause thymocyte death (15–18). The increased production of the proinflammatory cytokines TNF (16) and IFN-α (19) has also been proposed. Although this increased apoptosis of the thymocytes is one of the mechanisms leading to thymic atrophy, the increased export of immature T cells (20) and the disturbance of thymic epithelia (19) have also been suggested.

We have previously shown that infection of C57BL/6 mice with a highly virulent strain of *Mycobacterium avium* (strain ATCC 25291 SmT) induces profound peripheral T cell depletion and premature thymic atrophy (21, 22) and that *M. avium* is able to progressively infect the thymus (23, 24). Because IFN-γ is a key molecule in peripheral lymphocyte loss, we aimed at analyzing

*Institute for Molecular and Cell Biology, University of Porto, 4150-180 Porto, Portugal; †Department of Biological Sciences, Faculty of Pharmacy, University of Porto, 4050-313 Porto, Portugal; ‡Life and Health Sciences Research Institute, School of Health Sciences, University of Minho, 4710-057 Braga, Portugal; §Instituto de Investigação em Ciências da Vida e Saúde/Biomateriais, Materiais Biodegradáveis e Biomiméticos, Portuguese Government Associate Laboratory, 4710-057 Braga/Guimarães, Portugal; and ¶Department of Pediatrics, Cincinnati Children's Hospital Medical Center, Cincinnati, OH 45229; and ‖University of Cincinnati College of Medicine, Cincinnati, OH 45229

[1]M.B. and P.B.-S. contributed equally to this work.

[2]Current address: Mycobacterial Group, Centenary Institute, Sydney, Australia.

Received for publication June 4, 2012. Accepted for publication July 27, 2012.

This work was supported by project Factores de Competitividade-01-0124-Fundo Europeu de Desenvolvimento Regional-011142 (reference PTDC/SAU-MII/099102/2008 and PTDC/SAU-MII/101663/2008) from the Fundação para a Ciência e a Tecnologia (Lisbon, Portugal). P.B.-S. was granted a Ph.D. fellowship by the Fundação para a Ciência e a Tecnologia. M.B.J. was funded through National Institutes of Health Grant R01HL091769.

Address correspondence and reprint requests to Prof. Rui Appelberg or Dr. Margarida Correia-Neves, Institute for Molecular and Cell Biology, Rua do Campo Alegre 823, 4150-180 Porto, Portugal (R.A.) or Life and Health Sciences Research Institute, Campus de Gualtar, Braga, Portugal (M.C.-N.). E-mail addresses: rappelb@ibmc.up.pt (R.A.) and mcorreianeves@ecsaude.uminho.pt (M.C.-N.)

The online version of this article contains supplemental material.

Abbreviations used in this article: DN, double-negative; DP, double-positive; dpi, days postinfection; ETP, early thymic precursor; GC, glucocorticoid; iNOS, inducible NO synthase; SP, single-positive; WT, wild-type.

the role of this cytokine in mycobacterial infection-induced thymic atrophy. Moreover, IFN-γ is known to cause the upregulation of the inducible NO synthase (iNOS) in mycobacterial infection (25), and NO has been shown to synergize with corticosterone in the induction of apoptosis of thymocytes in in vitro experiments (26). Thus, we also aimed at determining if NO was leading to thymic atrophy during mycobacterial infection. IFN-γ–induced macrophage activation and the resulting increase in iNOS activity were identified as a major mechanism responsible for *M. avium*-induced thymic involution. Moreover, we show that IFN-γ–induced thymic atrophy synergized with corticosterone signaling. Notably, infection with a low-virulence strain that also leads to iNOS upregulation through IFN-γ activation did not lead to thymic atrophy suggesting that corticosterone upregulation is essential for infection-induced thymic atrophy. Finally, we provide evidence that the earliest steps of T cell differentiation might also be compromised.

Materials and Methods

Mice, infection, and thymectomy

C57BL/6 wild-type (WT) mice were purchased from Charles River Laboratories (Barcelona, Spain). IFN-γ–deficient C57BL/6 (IFN-γ KO) mice were bred in our facilities from a breeding pair purchased from The Jackson Laboratory (Bar Harbor, ME). Transgenic mice with a selective impairment in IFN-γ signaling in macrophages (MIIG) (27) were bred at the Institute for Molecular and Cell Biology (University of Porto, Porto, Portugal) from a breeding pair provided by the Cincinnati Children's Hospital Medical Center and the University of Cincinnati College of Medicine (Cincinnati, OH). iNOS-deficient C57BL/6 mice (iNOS KO) (28) were bred in our facilities after back-crossing the original strain (kindly provided by Drs. J. Mudgett, J.D. MacMicking, and C. Nathan, Cornell University, New York, NY) onto a C57BL/6 background for seven generations.

Eight- to ten-week-old female mice were infected i.v. with 10^6 CFU of the highly virulent *M. avium* strain ATCC 25291 SmT (obtained from the American Type Culture Collection, Manassas, VA) or the low-virulence strain 2447 (provided by Dr. F. Portaels, Institute of Tropical Medicine, Antwerp, Belgium) through a lateral tail vein. Bacterial inocula were prepared as described previously (21). The bacterial load in the organs was determined as previously described (23). Although no signs of distress were observed for the first 2 mo upon infection, some animals showed signs of deterioration of body condition in a non-synchronous way. To avoid excessive and unnecessary suffering of animals, humane endpoints were applied. Mice were sacrificed when reaching 25% weight loss.

Thymectomy or sham thymectomy surgical procedures were performed on anesthetized 8-wk-old mice 2 wk prior to infection. The thymi were removed by aspiration through a supra-sternum incision.

All animal experiments were performed in accordance with the recommendations of the European Convention for the Protection of Vertebrate Animals Used for Experimental and Other Scientific Purposes (ETS 123) and 86/609/EEC Directive and Portuguese rules (DL 129/92). The animal experimental protocol was approved by the competent national authority Direcção Geral de Veterinária.

Cell preparation

Spleens and thymi were collected and processed individually. Cell suspensions were obtained by gentle mechanical dissociation in PBS containing 3% FCS. RBCs were lysed using a hemolytic solution (155 mM NH_4Cl, 10 mM $KHCO_3$, pH 7.2) for 4 min at room temperature, and cells were resuspended in DMEM supplemented with 10% heat-inactivated FCS, 10 mM HEPES, 1 mM sodium pyruvate, 2 mM L-glutamine, 50 μg/ml streptomycin, and 50 U/ml penicillin (all from Invitrogen Life Technologies). The number of viable cells was counted by trypan blue exclusion using a hemocytometer.

Histology

Thymi were fixed on paraformaldehyde (4% in PBS) and embedded in paraffin. Thymic sections (2–3 μm) were stained by the Ziehl–Neelsen technique. Slides were visualized using an epifluorescence microscope (BX61 microscope) and photographed with an Olympus DP70 camera.

Flow cytometry

For the flow cytometry analysis of splenocytes, 10^6 cells were stained with FITC-conjugated anti-CD4 (RM4-5) or anti-CD19 (6D5) and PE-conjugated anti-CD8 (53-6.7). Propidium iodide (Sigma-Aldrich) was added at a final concentration of 1 μg/ml to allow the exclusion of dead cells. For thymocyte analysis, 10^6 thymic cells were labeled with distinct combinations of the following Abs: FITC or allophycocyanin-conjugated anti-CD3 (145-2C11), PE–Cy5.5 or V450-conjugated anti-CD4 (RM4-5), PE or V500-conjugated anti-CD8 (53-6.7), PerCP–Cy5.5–conjugated anti-CD24 (M1/69), allophycocyanin–Cy7–conjugated anti-CD25 (PC61), PE–Cy7–conjugated anti-CD44 (IM7), and PE-conjugated anti–c-Kit (2B8). For Lin, the following Abs were used conjugated with the same fluorochrome (FITC): anti-CD19 (6D5), anti-B220 (RA3-6B2), anti-CD11b (M1/70), anti-CD11c (N418), anti-NK1.1 (PK136), anti-Gr1 (RB6-8C5), anti-TER119 (TER119). All Abs were purchased from BioLegend (San Diego, CA) except the V450-conjugated anti-CD4 (RM4-5) and the V500-conjugated anti-CD8 (53-6.7), which were obtained from BD Biosciences. The acquisition of the spleen or thymus cell populations was performed on a FACSCalibur flow cytometer using CellQuest software (BD Biosciences), on an LSRII, or on a FACSCanto II flow cytometer using BD FACSDiva software (BD Biosciences). Data were analyzed using FlowJo software (Tree Star, Ashland, OR).

Blockage of glucocorticoid receptors

Mifepristone (RU486; Sigma-Aldrich), a synthetic glucocorticoid receptor antagonist, was dissolved in sterile polyethylene glycol 400 (Sigma-Aldrich) at a concentration of 5 mg/ml. Treatment was initiated by daily s.c. injections of either RU486 (25 mg/kg; 0.1 ml volume) or an equivalent volume of polyethylene glycol 400 (vehicle-treated mice) 1 d prior to infection until day 12 postinfection. This dose was previously shown to be effective in the reversion of corticosterone-dependent lymph node atrophy in stressed and influenza-infected mice (29, 30). From days 13 to 74 postinfection, mice were treated daily by i.p. injection with either RU486 (2.5 mg/kg; 0.2 ml volume) or an equivalent volume of vehicle. The RU486 solution for i.p. injections was obtained by dissolving RU486 in DMSO (Sigma-Aldrich) at a concentration of 50 mg/ml. This DMSO stock solution was diluted 1/10 with 1 M acetic acid just prior to use and then diluted again in PBS/BSA to a final concentration of 250 μg/ml.

Determination of serum corticosterone level

To obtain the serum concentration of corticosterone at basal levels, blood samples were obtained at 9 AM from a venous incision at the tip of the tail during a period not exceeding 2 min for each mouse, to avoid corticosterone sera level increase due to handling. Sera were collected and stored at −80°C until assayed for corticosterone by RIA using a ^{125}I RIA Kit (MP Biomedicals). Corticosterone levels were determined from a standard curve and expressed in nanograms per milliliter.

Dexamethasone sensitivity test

Control or infected mice were treated i.p. with dexamethasone (Oradexon; Organon, Oss, The Netherlands) at 0.1, 1.0, and 4.0 mg/kg or PBS (PBS-treated animals) 24 h before sacrifice. Mice were sacrificed at day 50 postinfection, and organs were removed for analysis. Thymocyte suspensions were obtained and analyzed by flow cytometry as described earlier.

Statistical analysis

Results were expressed as mean + SD. Statistical significance was calculated by using the two-tailed Student *t* test for data presented on Fig. 2A and the one-way ANOVA on all the other figures. The p values <0.05 were considered statistically significant.

Results

Severe thymic atrophy occurs in mice infected with the highly virulent M. avium *strain but not in mice infected with the low-virulence* M. avium *strain*

We compared the fate of the thymus in WT mice intravenously infected with a low-virulence strain of *M. avium* (strain 2447) and that of the thymus in mice infected with the highly virulent strain of *M. avium* (strain 25291). As shown in Fig. 1A–C, the size, weight, and cellularity of thymi from mice infected with *M. avium* 2447 did not differ from those of thymi of noninfected animals up to 80 days postinfection (dpi). Infection with strain 25291 led to a progressive shrinking of the organ, accompanied by a drastic reduction of its weight and cellularity. Flow cytometry analysis of the major thymocyte populations revealed no differences in thymi of mice infected with the low-virulence strain compared with thymi from noninfected controls (Fig. 1D–F). Infection with the highly

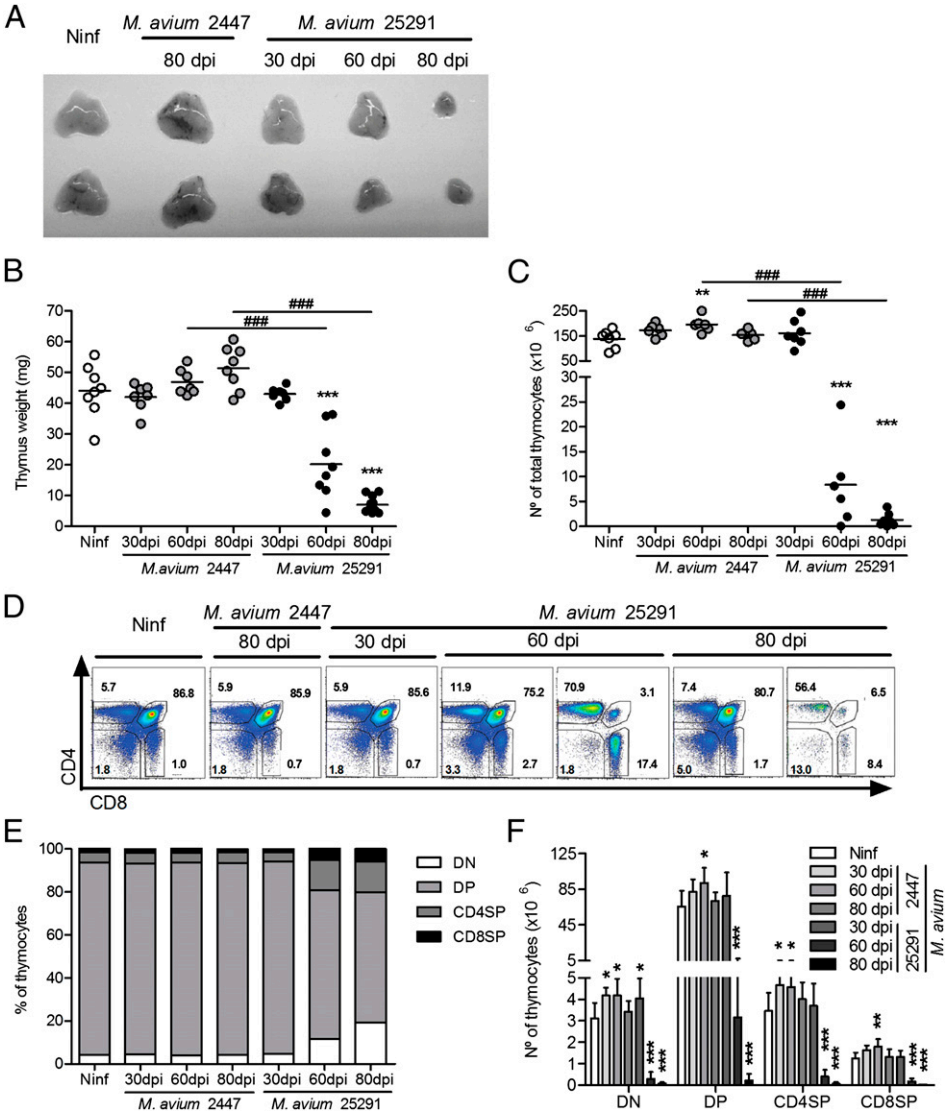

FIGURE 1. Infection with the highly virulent *M. avium* strain 25291 but not with the low-virulence strain 2447 induces strong thymus atrophy. (**A**) Photographs of thymi from uninfected WT mice (Ninf) and WT mice infected with *M. avium* strains 2447 or 25291 at the indicated time points. (**B** and **C**) Thymus weight and number of thymocytes from control noninfected (Ninf) mice and animals infected with strains 2447 or 25291. (**D**) Representative plots of anti-CD4 and anti-CD8 staining of thymi from control noninfected (Ninf) mice and mice infected with strains 2447 or 25291. The numbers indicate the percentage of cells in each region. (**E** and **F**) Percentage and number of thymic populations from control noninfected (Ninf) mice and animals infected with strains 2447 or 25291. Data represent the mean of the percentages or the mean and SD of the numbers of cells. Each group of noninfected mice comprised three to four animals, and each group of infected mice comprised seven animals analyzed individually. Data presented represent one experiment of three. $^{*}p < 0.05$, $^{**}p < 0.01$, $^{***}p < 0.001$ (statistically significant differences between infected and noninfected mice); $^{\#\#\#}p < 0.001$ (statistically significant differences between infected groups).

virulent strain led to changes in the relative proportions and total counts of double-negative (DN; $CD4^{-}CD8^{-}$), double-positive (DP; $CD4^{+}CD8^{+}$), and single-positive (SP; $CD4^{+}CD8^{-}$ or $CD4^{-}CD8^{+}$) populations. Thymic involution was somehow asynchronous with some mice exhibiting initial signs of thymic dysfunction sooner than others, as revealed by some variability in the pattern of thymocyte flow cytometry 60 dpi, illustrated in Fig. 1D. On average, the cells exhibiting a greater relative depletion were the DP populations (Fig. 1E) although all populations underwent massive loss from day 60 up to day 80 postinfection (Fig. 1F). This thymic atrophy was associated with increased bacterial loads within the thymus (Fig. 2A) in mice infected with the highly virulent strain, in agreement with what has been described for other organs (21, 22). Histologically, increasing numbers of acid-fast bacilli were detected, and progressive loss of the thymic structure was observed in samples taken from mice infected with the highly virulent strain, but no significant alterations were found in thymi from mice infected with the low-virulence strain up to 80 dpi (Fig. 2B). As previously shown, mice infected with the highly virulent strain developed peripheral lymphopenia, which was not observed in the case of infection by strain 2447 (Supplemental Fig. 1A). Removal of the thymus prior to infection with strain 25291 caused a slight increase in the peripheral depletion of T cells (Supplemental Fig. 1B) suggesting that thymic atrophy may have minor additive effects on the development of peripheral lymphopenia.

Thymic atrophy induced by M. avium *infection is IFN-γ dependent and mediated by NO*

IFN-γ is a key cytokine in the protective immune response against mycobacterial infection (31, 32) but has also been shown to participate in the induction of peripheral lymphopenia associated with *M. avium* 25291 infection (21, 22). To determine if IFN-γ was also implicated in *M. avium* infection thymic atrophy, we analyzed the thymi of IFN-γ KO mice during infection by strain 25291. As shown in Fig. 3A, mice that are unable to produce IFN-γ exhibited no thymic atrophy despite having similar mycobacterial burdens (7.9 ± 0.5 and 8.0 ± 0.4 $\log_{10}$ CFU/thymus in WT and IFN-γ KO mice, respectively, at 70 dpi). This observation shows that IFN-γ is essential for thymic atrophy during *M. avium* 25291 infection. Although essential for the depletion of lymphocytes at the periphery, IFN-γ was shown not to act directly on T cells as the loss of these latter cells occurred in chimeric mice whose T cells lacked the receptor for IFN-γ (22). The most likely candidate for an IFN-γ–responsive effector cell mediating lymphocyte or thymocyte loss is the macrophage. Thus, we infected "macrophage insensitive to IFN-γ" (MIIG) mice, whose CD68-expressing cells (mostly macrophages) do not respond to IFN-γ (27). In four

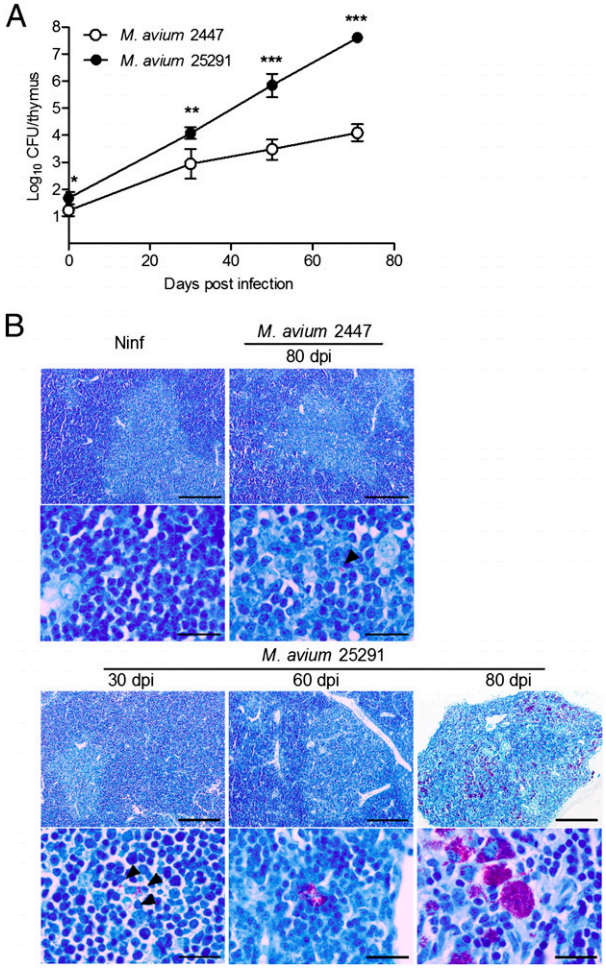

FIGURE 2. Infection with *M. avium* strain 25291 leads to higher bacterial loads in the thymus compared with infection with strain 2447. (**A**) Representative kinetics of *M. avium* infection of the thymus from WT mice inoculated with strains 2447 or 25291. Data represent the mean and SD of CFU from five mice per group from one of three experiments. $^{*}p < 0.05$, $^{**}p < 0.01$, $^{***}p < 0.001$ (statistically significant differences between mice infected with strains 2447 and 25291). (**B**) Representative thymic sections from noninfected mice (Ninf) and mice infected with strains 2447 or 25291 stained for acid-fast bacteria (Ziehl–Neelsen method). Scale bars represent 200 μm in the low-power views and 20 μm in the high-magnification images. Arrowheads indicate acid-fast bacteria in cases of low infection burden.

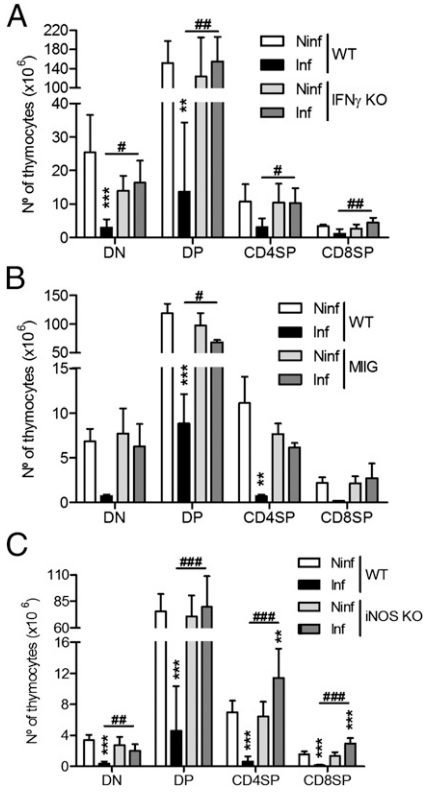

FIGURE 3. Thymus atrophy depends on IFN-γ production, IFN-γ–dependent macrophage activation, and NO production. (**A**) Number of cells of the thymic populations from WT or IFN-γ KO mice, either noninfected or infected with *M. avium* 25291 at 75 dpi. (**B**) Number of cells of the thymic populations from WT or MIIG transgenic mice, either noninfected or infected with *M. avium* 25291 at 80 dpi. (**C**) Number of cells of the thymic populations from WT or iNOS KO mice, either noninfected or infected with *M. avium* 25291 at 80 dpi. Data represent the mean and SD of the numbers of cells. Each group of mice comprised three to seven animals analyzed individually. Data shown represent one of three experiments. $^{**}p < 0.01$, $^{***}p < 0.001$ (statistically significant differences between infected and noninfected mice); $^{\#}p < 0.05$, $^{\#\#}p < 0.01$, $^{\#\#\#}p < 0.001$ (statistically significant differences between infected groups). Ninf, Noninfected.

independent experiments, control WT mice showed consistent thymic atrophy, ranging from 86 to 98% depletion of thymic cells during infection with strain 25291, whereas MIIG mice showed partial protection with 66% ($p < 0.05$), 27% (not statistically significant), 29% (not statistically significant), and 74% (not statistically significant) depletion of thymic cells. Fig. 3B shows the data of one of the experiments where subpopulations were analyzed and where no statistically significant differences were found. These data show that the macrophage is one of the cell types mediating thymocyte loss.

One of the major consequences of the activation of macrophages by IFN-γ is the increased production of NO due to the increased expression of iNOS. To assess the possible role of this reactive species in the induction of thymic atrophy, we infected iNOS-deficient animals with strain 25291. As shown in Fig. 3C, iNOS KO mice did not develop atrophy of the thymus. Notably, the bacterial load within the thymus was almost the same between WT and iNOS-deficient mice (7.7 and 7.5 $\log_{10}$ CFU/thymus in WT and iNOS KO mice, respectively, at 80 dpi).

Glucocorticoids cooperate with NO in the induction of thymic atrophy

As increased levels of glucocorticoids (GCs) are widely recognized as a common cause for increased thymocyte apoptosis during infection (16–18), we questioned whether corticosteroids were necessary for *M. avium*-induced thymic atrophy. Mice infected with strain 25291 but not those infected by strain 2447 showed slightly increased serum levels of corticosterone at 60 and 80 dpi (Fig. 4A). The increase in corticosterone induced by the highly virulent strain of *M. avium* was observed both in control WT mice and in IFN-γ–deficient mice showing that corticosteroids on their own were not sufficient to induce the atrophy of the thymus. To assess the biological role of this hormone in thymic atrophy, mice were infected with strain 25291 and treated daily with a steroid receptor type II antagonist (RU486) throughout the period of *M. avium* infection. In one experiment, the RU486 treatment of infected mice partially reverted the atrophy of the thymus, whereas in the second experiment, such reversion was complete (Fig. 4B) compared with vehicle-treated controls. No effect of RU486 on peripheral lymphopenia was observed in either experiment (data not shown).

Given that corticosterone blood levels showed only minor increases between *M. avium* 25291-infected and control noninfected mice and that, in contrast, RU486 treatment was quite active in

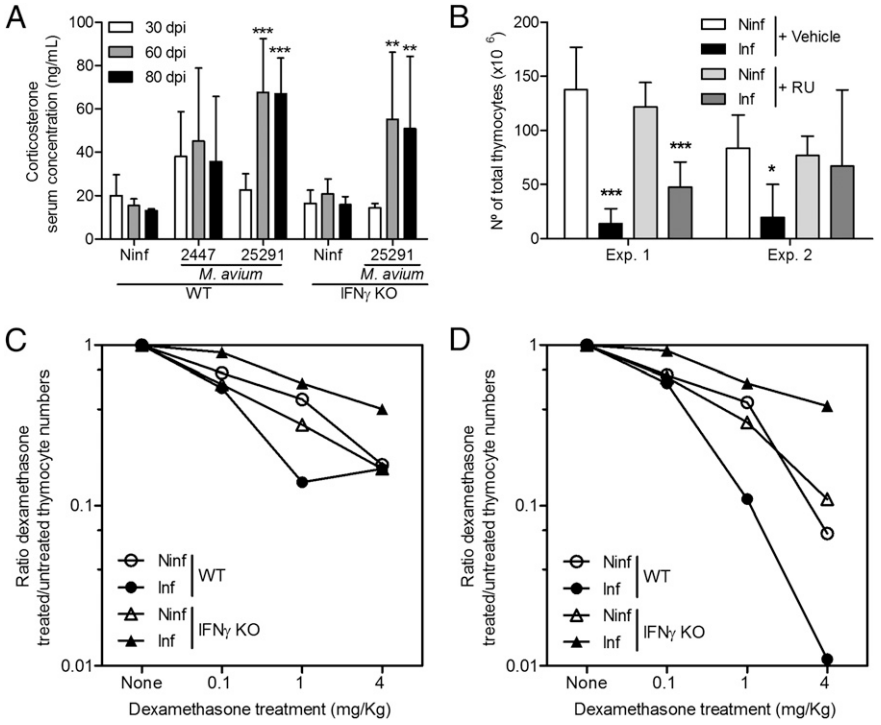

FIGURE 4. GCs are involved in the induction of thymus atrophy during infection with *M. avium* strain 25291. (**A**) Representative kinetics of serum corticosterone levels in WT mice infected with *M. avium* 25291 or 2447 compared with noninfected mice or of IFN-γ KO mice infected with strain 25291 versus noninfected. (**B**) Number of thymocytes from noninfected mice and mice infected for 75 d with *M. avium* 25291 and treated with either vehicle or RU486 (RU). Data represent the mean and SD of values obtained from six to eight mice in each group analyzed individually and represent two independent experiments. $*p < 0.05$, $**p < 0.01$, $***p < 0.001$ (statistically significant differences between infected and noninfected mice). (**C** and **D**) Decrease of total (C) and DP (D) thymocytes after dexamethasone treatment of noninfected or *M. avium* 25291-infected animals of either WT or IFN-γ KO strains. Data represent the ratio between the cell numbers in dexamethasone-treated animals and the cell numbers in PBS-treated animals (i.e., the fraction of cells remaining after dexamethasone treatment). Ninf, Noninfected.

preventing thymic atrophy in infected animals, we next investigated if thymocytes became more sensitive to apoptosis-inducing stimuli during infection by the highly virulent strain of *M. avium*. To that purpose, control and infected mice were administered dexamethasone, known to induce extensive cell death via corticosteroid receptor activation (33). Because IFN-γ KO mice do not exhibit thymic atrophy, we compared the effects of dexamethasone in both IFN-γ KO and WT animals. Mice were given increasing doses of dexamethasone (0.1, 1.0, and 4.0 mg/kg) 24 h before sacrifice at 50 dpi and compared with noninfected controls treated in a similar way. We observed a dose-dependent decrease of total and DP cells in both infected and noninfected WT and IFN-γ KO mice (Fig. 4C, 4D). Thymocyte loss was exacerbated by infection in WT mice but not in IFN-γ KO animals showing that IFN-γ production during infection increases thymocyte susceptibility to dexamethasone-induced cell death.

Impairment of the earliest stages of thymocyte development

To investigate further at what levels of thymocyte development the infection affects cell viability, we analyzed in detail DN thymocytes of mice infected with each *M. avium* strain. Whereas in mice infected with the low-virulence strain no differences were observed in the DN1–DN4 populations, animals infected with *M. avium* 25291 showed progressive reduction in cell numbers at all stages (Fig. 5A, 5B). The relative reduction in all stages was similar such that the proportions remained almost unchanged (Fig. 5A). We next analyzed what changes were found in *M. avium* 25291-infected mice that showed no thymic atrophy either because they were unable to produce IFN-γ, their macrophages did not respond to IFN-γ, or they do not express iNOS. No major alterations were induced by infection in IFN-γ KO or MIIG mice that exhibited normal or only slightly reduced numbers of DN1–DN4 subpopulations (Fig. 5C, 5D). Likewise, iNOS-deficient mice also maintained most of these subpopulations unchanged during infection except for DN2 (Fig. 5E). Finally, we analyzed the most immature thymocytes, the early thymic precursors (ETP), defined in the DN population as lineage-negative, $CD44^+$, $CD25^-$, and c-Kit^+ cells (see Supplemental Fig. 2 for a schematic representation of the gating strategy used to select this population). These cells were almost lost during infection of WT mice with the highly virulent strain of *M. avium* but not during infection with the strain 2447 (Fig. 6A, 6B). No loss was found in IFN-γ KO or MIIG mice infected with the highly virulent strain 25291 (Fig. 6C–F), but a statistically significant reduction was found in iNOS KO animals (Fig. 6G, 6H).

Discussion

In this study, we examined the mechanisms underlying the emergence of progressive thymic atrophy in mice infected with *M. avium* 25291. We showed that IFN-γ–deficient animals are resistant to the *M. avium*-induced thymic atrophy consistent with the fact that albeit essential for protective immunity against mycobacteria (31, 32), production of IFN-γ by T cells may not always be correlated with protection during infection by HIV or *Mycobacterium tuberculosis* (34–37). IFN-γ has been shown to be involved in the development of peripheral lymphopenia in mice infected with *M. avium* 25291 (22), to limit the exacerbated T cell activation responsible for immune pathology associated with granulomatous lesions (38), and to increase apoptosis of DP thymocytes (39). Furthermore, IFN-γ produced during measles virus infection not only inhibited cell proliferation but also disrupted the thymic epithelium responsible for thymocyte survival and differentiation into mature T cells, leading to thymic atrophy (40). Because IFN-γ does not act directly on lymphocytes in the periphery to induce their demise (22), and macrophages accumulate in large numbers in tissue granulomas and in the thymus of *M. avium*-infected mice (23, 24), we assessed the involvement of these phagocytes in the IFN-γ–mediated atrophy of the thymus. MIIG mice have macrophages (defined as CD68-expressing cells) that do not respond to IFN-γ and were found in this study not to develop thymic atrophy. This shows that macrophages respond to IFN-γ and mediate to a great extent the involution of the organ. Because IFN-γ–activated macrophages secrete important quantities of NO, we next evaluated the fate of the thymus in iNOS-deficient animals infected with strain 25291. These mice showed no evidence of thymic atrophy.

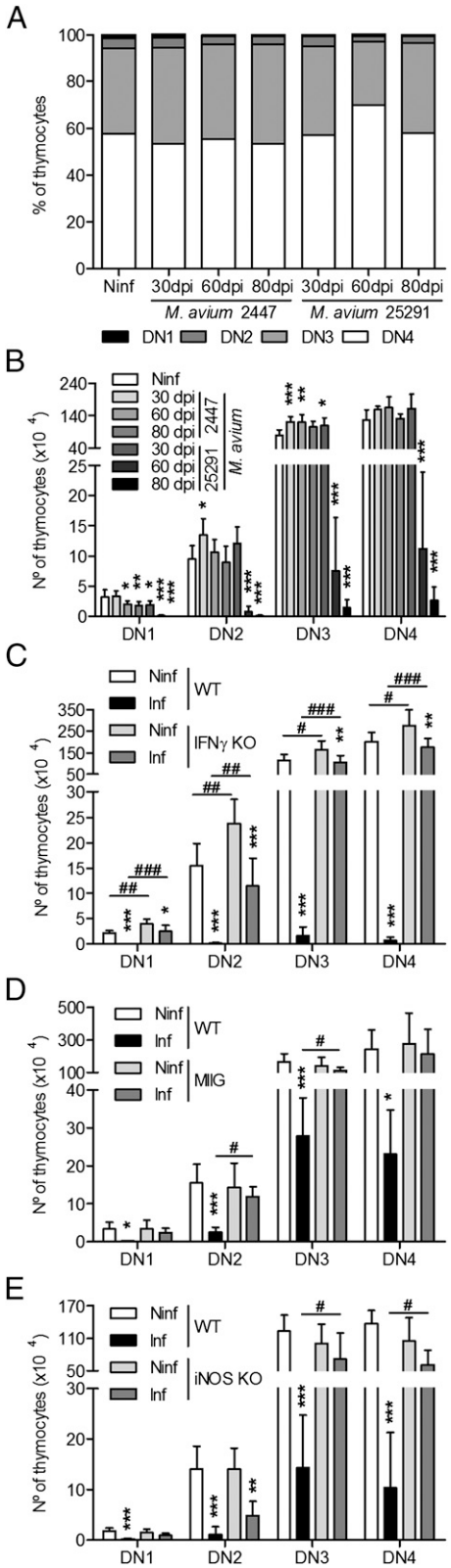

FIGURE 5. Infection with *M. avium* strain 25291 induces depletion of all subpopulations of DN thymocytes, which depends on IFN-γ production, IFN-γ–dependent macrophage activation, and NO production. (**A** and **B**) Percentage and number of DN thymic subpopulations from noninfected mice and mice infected with strains 2447 or 25291. (**C**) Number of DN thymic subpopulations from WT and IFN-γ KO mice, either noninfected or infected with *M. avium* 25291 at 80 dpi. (**D**) Number of DN thymic subpopulations from WT and MIIG mice, either noninfected or infected with *M. avium* 25291 at 80 dpi. (**E**) Number of DN thymic subpopulations from WT and iNOS KO mice, either noninfected or infected with *M. avium* 25291 at 80 dpi. Data represent the mean and SD of the number of cells. Each group of mice comprised three to six animals analyzed individually. Data shown represent one experiment of three. $^{*}p < 0.05$, $^{**}p < 0.01$, $^{***}p < 0.001$ (statistically significant differences between infected and control mice); $^{\#}p < 0.05$, $^{\#\#}p < 0.01$, $^{\#\#\#}p < 0.001$ (statistically significant differences between infected groups). Ninf, Noninfected.

Thus, a major pathway leading to thymic atrophy is dependent on the induction of iNOS expression in macrophages by IFN-γ produced in response to infection. NO has already been shown to be important in limiting T cell activity and survival at the periphery during mycobacterial infections (38), but this is the first demonstration, to our knowledge, of its activity in the thymus of an infected animal.

The mycobacterial loads in the thymus of mice infected with strain 25291 were significantly higher than those of mice infected with strain 2447 raising the possibility that the mycobacteria might themselves be toxic for the thymic tissue. However, this is not supported by the fact that the bacterial loads in the thymi of infected WT mice, which undergo atrophy, were very similar to those found in IFN-γ–deficient or iNOS-deficient animals, which did not develop such atrophy. Moreover, *M. avium* is known to be relatively nontoxic as evidenced by the very high microbial burdens that can be observed in infected hosts and that are still compatible with their survival (41–43).

The most frequent mechanism implicated in infection-induced thymic atrophy is increased thymocyte apoptosis due to increased production of GCs (15–17, 44–46). For example, the severe thymic atrophy found in mice infected with *Trypanosoma cruzi* is caused by an increased production of GCs (17, 47). This can also be seen during *M. tuberculosis* infection (48) or in mice given an injection of *M. tuberculosis* cord factor (trehalose 6,6′-dimycolate) (49). The activity of GCs might also synergize with that of IFN-γ. IFN-γ is known to increase serum levels of TNF, which in turn induces thymocyte apoptosis and augments the susceptibility of thymocytes to GCs (50). Given the importance of GCs in thymic involution, we studied whether GCs were implicated in the depletion of thymocytes during *M. avium* infection. Indeed, the infection with the highly virulent strain led to an increase, albeit small, of serum corticosterone levels. To determine if this increase affected thymocyte numbers, we performed an in vivo functional assay using an antagonist of the GC receptor (RU486). In two independent experiments, RU486 partially or completely reversed *M. avium*-induced thymic atrophy. Furthermore, infection increased thymocyte depletion by dexamethasone with cells from WT animals being more susceptible than those of IFN-γ–deficient mice. These data show an increase in susceptibility to GC-mediated thymocyte elimination. Although it is unclear to what extent GCs are required for *M. avium*-induced thymic atrophy, we suggest that they do play at least a partial role. It is clear, however, that GCs on their own are not sufficient to induce *M. avium*-induced thymic atrophy and that they need to synergize with IFN-γ or IFN-γ–induced pathways. The source of the GCs that participate in thymic involution is unclear. It has been shown that the murine thymus itself is capable of producing GCs (51, 52), and it was suggested that thymic epithelial cells may be able to produce GCs that would act directly in thymocytes (53, 54). The mechanisms that underlie the IFN-γ dependence to GC sensitivity are also not known, although changes in the levels of Notch and Bcl-2 expression have been suggested (55). Further work is needed to clarify this issue.

Because thymocytes expand several orders of magnitude from incoming bone marrow-derived precursors, a reduction in early

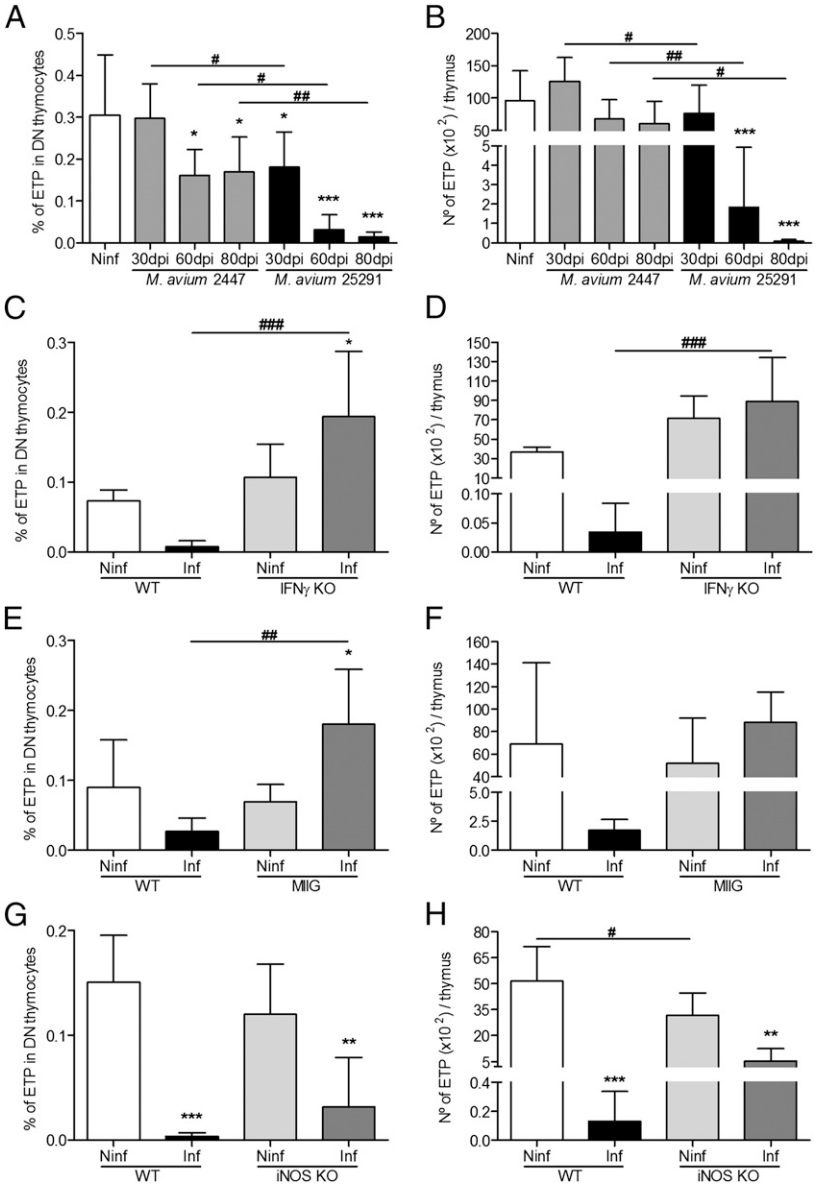

FIGURE 6. Infection with *M. avium* 25291 induces depletion of the early thymocyte precursors and depends on IFN-γ production, IFN-γ–dependent macrophage activation, and NO production. (**A** and **B**) Percentage (A) and number (B) of ETP from noninfected thymi and from thymi of WT mice infected with *M. avium* strains 2447 or 25291. (**C** and **D**) Percentage (C) and number (D) of ETP from noninfected thymi and from thymi of WT or IFN-γ KO mice infected with *M. avium* 25291 at 80 dpi. (**E** and **F**) Percentage (E) and number (F) of ETP from noninfected thymi and from thymi of WT or MIIG mice infected with *M. avium* 25291 at 80 dpi. (**G** and **H**) Percentage (G) and number (H) of ETP from noninfected thymi and from thymi of WT or iNOS KO mice infected with *M. avium* 25291 at 80 dpi. Data represent the mean of the percentages or the mean and SD of the number of cells. Each group of mice comprised three to six animals analyzed individually. Data shown represent one experiment of three. $^{*}p < 0.05$, $^{**}p < 0.01$, $^{***}p < 0.001$ (statistically significant differences between infected and noninfected control mice); $^{\#}p < 0.05$, $^{\#\#}p < 0.01$, $^{\#\#\#}p < 0.001$ (statistically significant differences between infected groups). Ninf, Noninfected.

thymic precursors could affect thymic cellularity. The progressive reduction in thymocyte numbers observed in this study was seen among the DN1 to the DN4 stages to an extent that was proportional to the relative abundance of these cells in a normal thymus. Furthermore, the most immature thymocytes (c-Kit^{+}, lin^{-} DN1 cells) were found to be severely deficient in advanced stages of thymic atrophy. These observations are consistent with several scenarios of thymocyte depletion: 1) it might occur predominantly in the thymus and affect all cell types, 2) there might be a predominant effect on the recently arrived precursors affecting the subsequent ability to expand inside the thymic tissue, or 3) a reduction in the release of precursors from the bone marrow might reduce thymus seeding. In this context, it has been shown that early lymphoid progenitors in mouse and man are highly sensitive to GCs (56), and alterations in chemokine expression and bone marrow retention phenomena are observed in HIV-infected patients (57). Our data with iNOS-deficient mice suggest that at least some of the reduction in thymocyte numbers is occurring locally in the thymus. iNOS-deficient mice showed a statistically significant reduction in the number of early thymocyte precursors suggesting that NO-independent mechanisms lead to the failure of the bone marrow to seed the thymus. Yet, despite the reduced seeding of the thymus by early thymocyte precursors, iNOS-deficient animals did not develop thymic atrophy indicating that NO may be required for local thymocyte death in the thymic tissue. The lower production of thymic precursors by the bone marrow might be due to the direct action of IFN-γ on hematopoietic stem cells or multipotent progenitors as has already been proposed (58–60). The fact that MIIG mice are not as well protected from thymocyte loss as IFN-γ–deficient mice suggests that IFN-γ may also act on cells other than the macrophage, namely the progenitor cells in the bone marrow. Although thymic emigrants are important for the maintenance of the peripheral lymphocyte pool (61–63) and the loss of thymic output may accelerate the loss of splenic T cells, as shown in this study in thymectomized mice (Supplemental Fig. 1B), we found that peripheral lymphopenia still occurs in situations where the thymus remains apparently intact such as in iNOS-deficient animals or when GC activity has been blocked by the receptor antagonist RU486 (data not shown).

In summary, the current report identifies the role of IFN-γ–activated macrophages and their ability to produce NO in the development of thymic atrophy most likely coadjuvanted by the increased susceptibility to GC-mediated thymocyte apoptosis that develops during infection with the highly virulent strain of *M. avium*

and suggests the possibility of a failure of the bone marrow to seed the thymus with precursors.

Disclosures

The authors have no financial conflicts of interest.

References

1. Savino, W. 2006. The thymus is a common target organ in infectious diseases. *PLoS Pathog.* 2: e62.
2. Lynch, H. E., G. L. Goldberg, A. Chidgey, M. R. Van den Brink, R. Boyd, and G. D. Sempowski. 2009. Thymic involution and immune reconstitution. *Trends Immunol.* 30: 366–373.
3. Vigano, A., S. Vella, M. Saresella, A. Vanzulli, D. Bricalli, S. Di Fabio, P. Ferrante, M. Andreotti, M. Pirillo, L. G. Dally, et al. 2000. Early immune reconstitution after potent antiretroviral therapy in HIV-infected children correlates with the increase in thymus volume. *AIDS* 14: 251–261.
4. Kalayjian, R. C., J. Spritzler, M. Pu, A. Landay, R. B. Pollard, V. Stocker, L. A. Harthi, B. H. Gross, I. R. Francis, S. A. Fiscus, et al; Adult AIDS Clinical Trials Group 5015 and 5113 Study Teams. 2005. Distinct mechanisms of T cell reconstitution can be identified by estimating thymic volume in adult HIV-1 disease. *J. Infect. Dis.* 192: 1577–1587.
5. Smith, K. Y., H. Valdez, A. Landay, J. Spritzler, H. A. Kessler, E. Connick, D. Kuritzkes, B. Gross, I. Francis, J. M. McCune, and M. M. Lederman. 2000. Thymic size and lymphocyte restoration in patients with human immunodeficiency virus infection after 48 weeks of zidovudine, lamivudine, and ritonavir therapy. *J. Infect. Dis.* 181: 141–147.
6. Eysteinsdottir, J. H., J. Freysdottir, A. Haraldsson, J. Stefansdottir, I. Skaftadottir, H. Helgason, and H. M. Ogmundsdottir. 2004. The influence of partial or total thymectomy during open heart surgery in infants on the immune function later in life. *Clin. Exp. Immunol.* 136: 349–355.
7. Prelog, M., M. Keller, R. Geiger, A. Brandstätter, R. Würzner, U. Schweigmann, M. Zlamy, L. B. Zimmerhackl, and B. Grubeck-Loebenstein. 2009. Thymectomy in early childhood: significant alterations of the CD4(+)CD45RA(+)CD62L(+) T cell compartment in later life. *Clin. Immunol.* 130: 123–132.
8. Aspinall, R., D. Pitts, A. Lapenna, and W. Mitchell. 2010. Immunity in the elderly: the role of the thymus. *J. Comp. Pathol.* 142(Suppl 1): S111–S115.
9. Vezys, V., D. Masopust, C. C. Kemball, D. L. Barber, L. A. O'Mara, C. P. Larsen, T. C. Pearson, R. Ahmed, and A. E. Lukacher. 2006. Continuous recruitment of naive T cells contributes to heterogeneity of antiviral CD8 T cells during persistent infection. *J. Exp. Med.* 203: 2263–2269.
10. Sauce, D., and V. Appay. 2011. Altered thymic activity in early life: how does it affect the immune system in young adults? *Curr. Opin. Immunol.* 23: 543–548.
11. Gagnerault, M. C., O. Lanvin, V. Pasquier, C. Garcia, D. Damotte, B. Lucas, and F. Lepault. 2009. Autoimmunity during thymectomy-induced lymphopenia: role of thymus ablation and initial effector T cell activation timing in nonobese diabetic mice. *J. Immunol.* 183: 4913–4920.
12. Song, F., Z. Guan, I. E. Gienapp, T. Shawler, J. Benson, and C. C. Whitacre. 2006. The thymus plays a role in oral tolerance in experimental autoimmune encephalomyelitis. *J. Immunol.* 177: 1500–1509.
13. AbuAttieh, M., D. Bender, E. Liu, P. Wettstein, J. L. Platt, and M. Cascalho. 2012. Affinity maturation of antibodies requires integrity of the adult thymus. *Eur. J. Immunol.* 42: 500–510.
14. Corbeau, P., and J. Reynes. 2011. Immune reconstitution under antiretroviral therapy: the new challenge in HIV-1 infection. *Blood* 117: 5582–5590.
15. Wang, D., N. Müller, K. G. McPherson, and H. M. Reichardt. 2006. Glucocorticoids engage different signal transduction pathways to induce apoptosis in thymocytes and mature T cells. *J. Immunol.* 176: 1695–1702.
16. Chen, W., R. Kuolee, J. W. Austin, H. Shen, Y. Che, and J. W. Conlan. 2005. Low dose aerosol infection of mice with virulent type A *Francisella tularensis* induces severe thymus atrophy and CD4+CD8+ thymocyte depletion. *Microb. Pathog.* 39: 189–196.
17. Pérez, A. R., E. Roggero, A. Nicora, J. Palazzi, H. O. Besedovsky, A. Del Rey, and O. A. Bottasso. 2007. Thymus atrophy during *Trypanosoma cruzi* infection is caused by an immuno-endocrine imbalance. *Brain Behav. Immun.* 21: 890–900.
18. Leite de Moraes, M. C., M. Hontebeyrie-Joskowicz, F. Leboulenger, W. Savino, M. Dardenne, and F. Lepault. 1991. Studies on the thymus in Chagas' disease. II. Thymocyte subset fluctuations in *Trypanosoma cruzi*-infected mice: relationship to stress. *Scand. J. Immunol.* 33: 267–275.
19. Papadopoulou, A. S., J. Dooley, M. A. Linterman, W. Pierson, O. Ucar, B. Kyewski, S. Zuklys, G. A. Hollander, P. Matthys, D. H. Gray, et al. 2012. The thymic epithelial microRNA network elevates the threshold for infection-associated thymic involution via miR-29a mediated suppression of the IFN-α receptor. *Nat. Immunol.* 13: 181–187.
20. Morrot, A., E. Terra-Granado, A. R. Pérez, S. D. Silva-Barbosa, N. M. Milićević, D. A. Farias-de-Oliveira, L. R. Berbert, J. De Meis, C. M. Takiya, J. Beloscar, et al. 2011. Chagasic thymic atrophy does not affect negative selection but results in the export of activated CD4+CD8+ T cells in severe forms of human disease. *PLoS Negl. Trop. Dis.* 5: e1268.
21. Flórido, M., A. S. Gonçalves, R. A. Silva, S. Ehlers, A. M. Cooper, and R. Appelberg. 1999. Resistance of virulent *Mycobacterium avium* to gamma interferon-mediated antimicrobial activity suggests additional signals for induction of mycobacteriostasis. *Infect. Immun.* 67: 3610–3618.
22. Flórido, M., J. E. Pearl, A. Solache, M. Borges, L. Haynes, A. M. Cooper, and R. Appelberg. 2005. Gamma interferon-induced T-cell loss in virulent *Mycobacterium avium* infection. *Infect. Immun.* 73: 3577–3586.
23. Nobrega, C., P. J. Cardona, S. Roque, P. Pinto do O, R. Appelberg, and M. Correia-Neves. 2007. The thymus as a target for mycobacterial infections. *Microbes Infect.* 9: 1521–1529.
24. Nobrega, C., S. Roque, C. Nunes-Alves, A. Coelho, I. Medeiros, A. G. Castro, R. Appelberg, and M. Correia-Neves. 2010. Dissemination of mycobacteria to the thymus renders newly generated T cells tolerant to the invading pathogen. *J. Immunol.* 184: 351–358.
25. Flesch, I. E., and S. H. Kaufmann. 1990. Activation of tuberculostatic macrophage functions by gamma interferon, interleukin-4, and tumor necrosis factor. *Infect. Immun.* 58: 2675–2677.
26. Cohen, O., S. Kfir-Erenfeld, R. Spokoini, Y. Zilberman, E. Yefenof, and R. V. Sionov. 2009. Nitric oxide cooperates with glucocorticoids in thymic epithelial cell-mediated apoptosis of double positive thymocytes. *Int. Immunol.* 21: 1113–1123.
27. Lykens, J. E., C. E. Terrell, E. E. Zoller, S. Divanovic, A. Trompette, C. L. Karp, J. Aliberti, M. J. Flick, and M. B. Jordan. 2010. Mice with a selective impairment of IFN-gamma signaling in macrophage lineage cells demonstrate the critical role of IFN-gamma-activated macrophages for the control of protozoan parasitic infections in vivo. *J. Immunol.* 184: 877–885.
28. MacMicking, J. D., C. Nathan, G. Hom, N. Chartrain, D. S. Fletcher, M. Trumbauer, K. Stevens, Q. W. Xie, K. Sokol, N. Hutchinson, et al. 1995. Altered responses to bacterial infection and endotoxic shock in mice lacking inducible nitric oxide synthase. *Cell* 81: 641–650.
29. Dobbs, C. M., M. Vasquez, R. Glaser, and J. F. Sheridan. 1993. Mechanisms of stress-induced modulation of viral pathogenesis and immunity. *J. Neuroimmunol.* 48: 151–160.
30. Dobbs, C. M., N. Feng, F. M. Beck, and J. F. Sheridan. 1996. Neuroendocrine regulation of cytokine production during experimental influenza viral infection: effects of restraint stress-induced elevation in endogenous corticosterone. *J. Immunol.* 157: 1870–1877.
31. Cooper, A. M., D. K. Dalton, T. A. Stewart, J. P. Griffin, D. G. Russell, and I. M. Orme. 1993. Disseminated tuberculosis in interferon gamma gene-disrupted mice. *J. Exp. Med.* 178: 2243–2247.
32. Flynn, J. L., J. Chan, K. J. Triebold, D. K. Dalton, T. A. Stewart, and B. R. Bloom. 1993. An essential role for interferon gamma in resistance to *Mycobacterium tuberculosis* infection. *J. Exp. Med.* 178: 2249–2254.
33. Purton, J. F., J. A. Monk, D. R. Liddicoat, K. Kyparissoudis, S. Sakkal, S. J. Richardson, D. I. Godfrey, and T. J. Cole. 2004. Expression of the glucocorticoid receptor from the 1A promoter correlates with T lymphocyte sensitivity to glucocorticoid-induced cell death. *J. Immunol.* 173: 3816–3824.
34. Draenert, R., C. L. Verrill, Y. Tang, T. M. Allen, A. G. Wurcel, M. Boczanowski, A. Lechner, A. Y. Kim, T. Suscovich, N. V. Brown, et al. 2004. Persistent recognition of autologous virus by high-avidity CD8 T cells in chronic, progressive human immunodeficiency virus type 1 infection. *J. Virol.* 78: 630–641.
35. Leal, I. S., B. Smedegård, P. Andersen, and R. Appelberg. 2001. Failure to induce enhanced protection against tuberculosis by increasing T-cell-dependent interferon-gamma generation. *Immunology* 104: 157–161.
36. Elias, D., H. Akuffo, and S. Britton. 2005. PPD induced in vitro interferon gamma production is not a reliable correlate of protection against *Mycobacterium tuberculosis*. *Trans. R. Soc. Trop. Med. Hyg.* 99: 363–368.
37. Majlessi, L., M. Simsova, Z. Jarvis, P. Brodin, M. J. Rojas, C. Bauche, C. Nouzé, D. Ladant, S. T. Cole, P. Sebo, and C. Leclerc. 2006. An increase in antimycobacterial Th1-cell responses by prime-boost protocols of immunization does not enhance protection against tuberculosis. *Infect. Immun.* 74: 2128–2137.
38. Cooper, A. M., L. B. Adams, D. K. Dalton, R. Appelberg, and S. Ehlers. 2002. IFN-gamma and NO in mycobacterial disease: new jobs for old hands. *Trends Microbiol.* 10: 221–226.
39. Kato, Y., A. Morikawa, T. Sugiyama, N. Koide, G. Z. Jiang, T. Lwin, T. Yoshida, and T. Yokochi. 1997. Augmentation of lipopolysaccharide-induced thymocyte apoptosis by interferon-gamma. *Cell. Immunol.* 177: 103–108.
40. Vidalain, P. O., D. Laine, Y. Zaffran, O. Azocar, C. Servet-Delprat, T. F. Wild, C. Rabourdin-Combe, and H. Valentin. 2002. Interferons mediate terminal differentiation of human cortical thymic epithelial cells. *J. Virol.* 76: 6415–6424.
41. Wong, B., F. F. Edwards, T. E. Kiehn, E. Whimbey, H. Donnelly, E. M. Bernard, J. W. Gold, and D. Armstrong. 1985. Continuous high-grade *mycobacterium avium-intracellulare* bacteremia in patients with the acquired immune deficiency syndrome. *Am. J. Med.* 78: 35–40.
42. Rathbun, R. C., E. S. Martin, III, V. E. Eaton, and E. B. Matthew. 1991. Current and investigational therapies for AIDS-associated *Mycobacterium avium* complex disease. *Clin. Pharm.* 10: 280–291.
43. Griffith, D. E. 2003. Emergence of nontuberculous mycobacteria as pathogens in cystic fibrosis. *Am. J. Respir. Crit. Care Med.* 167: 810–812.
44. Butts, C. L., and E. M. Sternberg. 2008. Neuroendocrine factors alter host defense by modulating immune function. *Cell. Immunol.* 252: 7–15.
45. Schwartzman, R. A., and J. A. Cidlowski. 1994. Glucocorticoid-induced apoptosis of lymphoid cells. *Int. Arch. Allergy Immunol.* 105: 347–354.
46. Chung, H. T., W. E. Samlowski, and R. A. Daynes. 1986. Modification of the murine immune system by glucocorticosteroids: alterations of the tissue localization properties of circulating lymphocytes. *Cell. Immunol.* 101: 571–585.
47. Roggero, E., A. R. Pérez, M. Tamae-Kakazu, I. Piazzon, I. Nepomnaschy, H. O. Besedovsky, O. A. Bottasso, and A. del Rey. 2006. Endogenous glucocorticoids

cause thymus atrophy but are protective during acute *Trypanosoma cruzi* infection. *J. Endocrinol.* 190: 495–503.
48. Bottasso, O., M. L. Bay, H. Besedovsky, and A. del Rey. 2007. The immuno-endocrine component in the pathogenesis of tuberculosis. *Scand. J. Immunol.* 66: 166–175.
49. Ozeki, Y., K. Kaneda, N. Fujiwara, M. Morimoto, S. Oka, and I. Yano. 1997. In vivo induction of apoptosis in the thymus by administration of mycobacterial cord factor (trehalose 6,6′-dimycolate). *Infect. Immun.* 65: 1793–1799.
50. Brouckaert, P., B. Everaerdt, and W. Fiers. 1992. The glucocorticoid antagonist RU38486 mimics interleukin-1 in its sensitization to the lethal and interleukin-6-inducing properties of tumor necrosis factor. *Eur. J. Immunol.* 22: 981–986.
51. Pazirandeh, A., Y. Xue, T. Prestegaard, M. Jondal, and S. Okret. 2002. Effects of altered glucocorticoid sensitivity in the T cell lineage on thymocyte and T cell homeostasis. *FASEB J.* 16: 727–729.
52. Lechner, O., G. J. Wiegers, A. J. Oliveira-Dos-Santos, H. Dietrich, H. Recheis, M. Waterman, R. Boyd, and G. Wick. 2000. Glucocorticoid production in the murine thymus. *Eur. J. Immunol.* 30: 337–346.
53. Pazirandeh, A., Y. Xue, I. Rafter, J. Sjövall, M. Jondal, and S. Okret. 1999. Paracrine glucocorticoid activity produced by mouse thymic epithelial cells. *FASEB J.* 13: 893–901.
54. Zilberman, Y., E. Zafrir, H. Ovadia, E. Yefenof, R. Guy, and R. V. Sionov. 2004. The glucocorticoid receptor mediates the thymic epithelial cell-induced apoptosis of CD4+8+ thymic lymphoma cells. *Cell. Immunol.* 227: 12–23.
55. Kong, F. K., C. L. Chen, and M. D. Cooper. 2002. Reversible disruption of thymic function by steroid treatment. *J. Immunol.* 168: 6500–6505.
56. Igarashi, H., K. L. Medina, T. Yokota, M. I. Rossi, N. Sakaguchi, P. C. Comp, and P. W. Kincade. 2005. Early lymphoid progenitors in mouse and man are highly sensitive to glucocorticoids. *Int. Immunol.* 17: 501–511.
57. Sauce, D., M. Larsen, S. Fastenackels, M. Pauchard, H. Ait-Mohand, L. Schneider, A. Guihot, F. Boufassa, J. Zaunders, M. Iguertsira, et al. 2011. HIV disease progression despite suppression of viral replication is associated with exhaustion of lymphopoiesis. *Blood* 117: 5142–5151.
58. Baldridge, M. T., K. Y. King, N. C. Boles, D. C. Weksberg, and M. A. Goodell. 2010. Quiescent haematopoietic stem cells are activated by IFN-gamma in response to chronic infection. *Nature* 465: 793–797.
59. MacNamara, K. C., M. Jones, O. Martin, and G. M. Winslow. 2011. Transient activation of hematopoietic stem and progenitor cells by IFNγ during acute bacterial infection. *PLoS ONE* 6: e28669.
60. de Bruin, A. M., S. F. Libregts, M. Valkhof, L. Boon, I. P. Touw, and M. A. Nolte. 2012. IFNγ induces monopoiesis and inhibits neutrophil development during inflammation. *Blood* 119: 1543–1554.
61. Berzins, S. P., R. L. Boyd, and J. F. Miller. 1998. The role of the thymus and recent thymic migrants in the maintenance of the adult peripheral lymphocyte pool. *J. Exp. Med.* 187: 1839–1848.
62. Berzins, S. P., D. I. Godfrey, J. F. Miller, and R. L. Boyd. 1999. A central role for thymic emigrants in peripheral T cell homeostasis. *Proc. Natl. Acad. Sci. USA* 96: 9787–9791.
63. Berzins, S. P., A. P. Uldrich, J. S. Sutherland, J. Gill, J. F. Miller, D. I. Godfrey, and R. L. Boyd. 2002. Thymic regeneration: teaching an old immune system new tricks. *Trends Mol. Med.* 8: 469–476.

Supplementary figures

Figure S1: Thymectomy slightly increases peripheral lymphopenia induced by infection with *M. avium* 25291.

A. Cellular composition of the spleens from non-infected (Ninf) mice and C57Bl/6 mice infected with *M. avium* 2447 or 25291 at 75 dpi. Data presented represent the mean and standard deviation of the number of cells and represents one experiment out of two with six mice analyzed individually in each group. Statistically significant differences between infected and control mice are labeled *p<0.05, ***p<0.001. Statistically significant differences between infected groups are labeled ###p<0.001. B. Cellular composition of the spleens of non-infected (Ninf) C57Bl/6 mice or *M. avium* 25291-infected C57Bl/6 mice at 90 dpi that either were subjected to sham surgery (SHAM) or were thymectomized (TX). Mice were infected i.v. with 10^6 *M. avium* 25291 two weeks after thymectomy. Data represent the mean and standard deviation of the number of cells and represents one experiment out of three with six mice in each group analyzed individually. Statistically significant differences between infected and control mice are labeled ***p <0.001. Statistically significant differences between non-infected (Ninf) SHAM and TX mice are labeled #p<0.05, ## p<0.01.

Figure S2: Schematic representation of the gating used to select thymic populations by flow cytometry.

A. The four main thymic populations were selected on the lymphocyte gate after elimination of duplets and lineage markers (lin) positive cells (cells expressing CD19,

B220, CD11b, CD11c, NK1.1, Gr1, and/or TER119), and according to the expression of CD4 and CD8 molecules: DN ($CD4^-CD8^-$), DP ($CD4^+CD8^+$); CD4SP ($CD4^+CD8^-$) and CD8SP ($CD4^-CD8^+$). B. The four DN subpopulations were selected on the DN gate as not expressing CD3 molecule and according to the expression of CD44 and CD25: DN1 ($CD44^+CD25^-$), DN2 ($CD44^+CD25^+$); DN3 ($CD44^-CD25^+$) and DN4 ($CD44^-CD25^-$). Early thymic precursors (ETP) were selected on the DN1 gate as the cells presenting high expression of cKit.

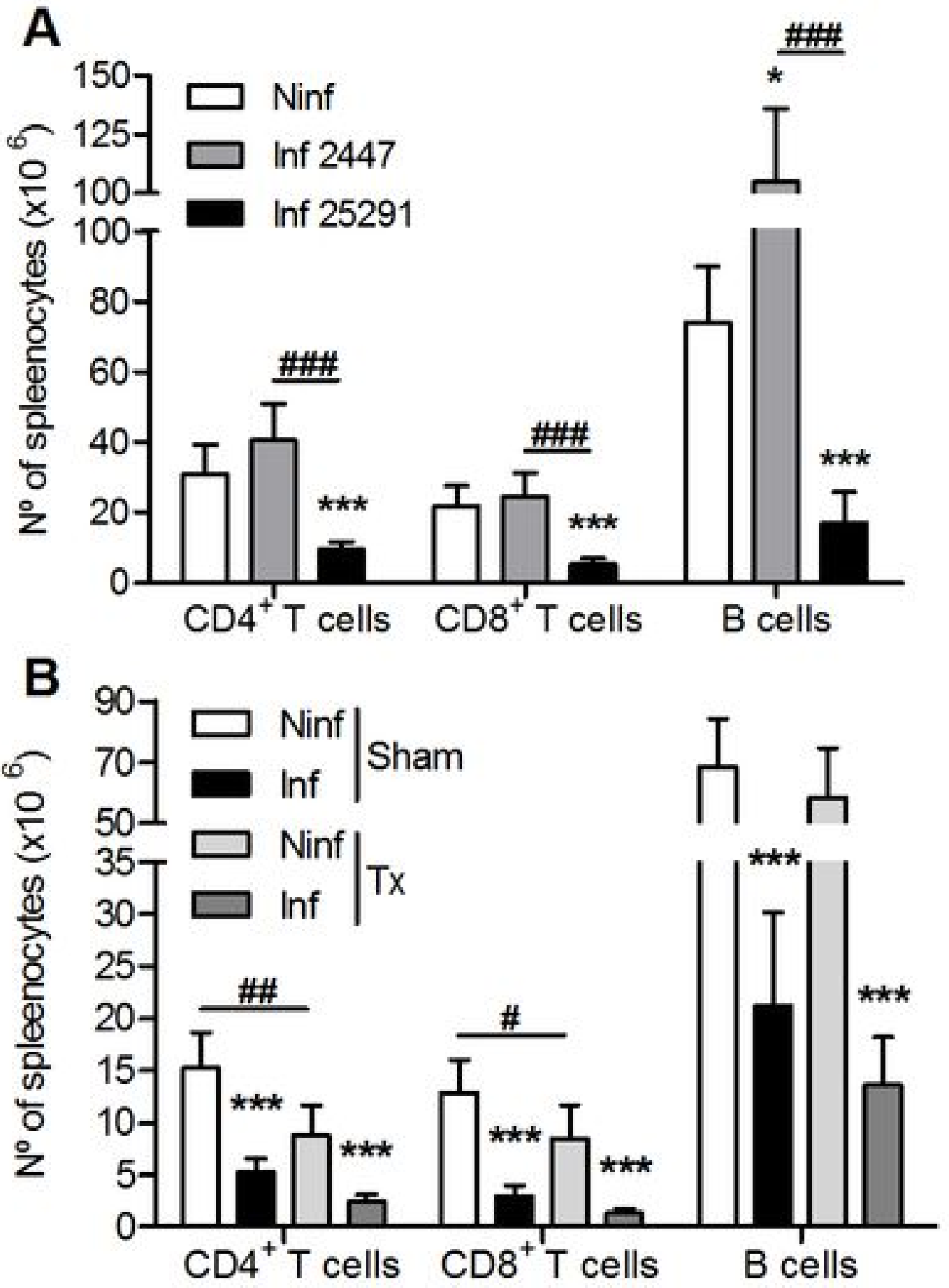
A
Nº of spleenocytes (x10 6)
150
125
100
100
80
60
40
20
0
Ninf
Inf 2447
Inf 25291
###
###
####
*
***
***
***
CD4+ T cells
CD8+ T cells
B cells
B
Nº of spleenocytes (x10 6)
90
70
50
35
30
25
20
15
10
5
0
Ninf
Inf
Sham
Ninf
Inf
Tx
##
#
***
***
***
***
***
CD4+ T cells
CD8+ T cells
B cells

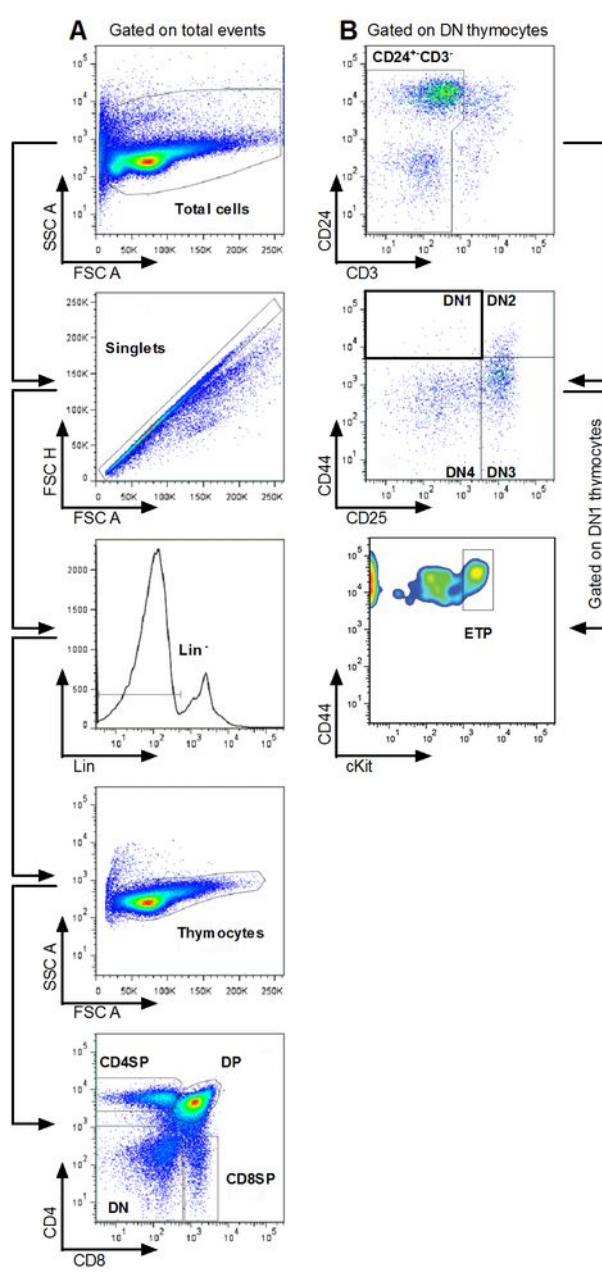
A
Gated on total events
Total cells
SSC A
FSC A
Singlets
FSC H
FSC A
Lin-
Lin
Thymocytes
SSC A
FSC A
CD4SP
DP
CD8SP
DN
CD4
CD8
B
Gated on DN thymocytes
CD24+CD3-
CD24
CD3
DN1
DN2
DN4
DN3
CD44
CD25
ETP
CD44
cKit
Gated on DN1 thymocytes